0022-3565/11/3362-506–515$20.00
THE JOURNAL OF PHARMACOLOGY AND EXPERIMENTAL THERAPEUTICS
JPET 336:506–515, 2011

Vol. 336, No. 2
172981/3660088
Printed in U.S.A.

The Distribution of Nifurtimox Across the Healthy and Trypanosome-Infected Murine Blood-Brain and Blood-Cerebrospinal Fluid Barriers

Sinthujah Jeganathan, Lisa Sanderson, Murat Dogruel, Jean Rodgers, Simon Croft, and Sarah A. Thomas

Pharmaceutical Sciences Research Division, King's College London, London, United Kingdom (S.J., L.S., M.D., S.A.T.); Division of Infection and Immunity, University of Glasgow Veterinary School, Glasgow, United Kingdom (J.R.); and London School of Hygiene and Tropical Medicine, University of London, London, United Kingdom (S.C.)

Received July 15, 2010; accepted November 2, 2010

ABSTRACT

Nifurtimox, an antiparasitic drug, is used to treat American trypanosomiasis (Chagas disease) and has shown promise in treating central nervous system (CNS)-stage human African trypanosomiasis (HAT; sleeping sickness). In combination with other antiparasitic drugs, the efficacy of nifurtimox against HAT improves, although why this happens is unclear. Studying how nifurtimox crosses the blood-brain barrier (BBB) and reaches the CNS may clarify this issue and is the focus of this study. To study the interaction of nifurtimox with the blood-CNS interfaces, we used the in situ brain/choroid plexus perfusion technique in healthy and trypanosome-infected mice and the isolated incubated choroid plexus. Results revealed that nifurtimox could cross the healthy and infected blood-brain and blood-cerebrospinal fluid (CSF) barriers (K_{in} brain parenchyma was 50.8 ± 9.0 $\mu l \cdot min^{-1} \cdot g^{-1}$). In fact, the loss of barrier integrity associated with trypanosome infection failed to change the distribution of [^{3}H]nifurtimox to any significant extent, suggesting there is not an effective paracellular barrier for [^{3}H]nifurtimox entry into the CNS. Our studies also indicate that [^{3}H]nifurtimox is not a substrate for P-glycoprotein, an efflux transporter expressed on the luminal membrane of the BBB. However, there was evidence of [^{3}H]nifurtimox interaction with transporters at both the blood-brain and blood-CSF barriers as demonstrated by cross-competition studies with the other antitrypanosomal agents, eflornithine, suramin, melarsoprol, and pentamidine. Consequently, CNS efficacy may be improved with nifurtimox-pentamidine combinations, but over time may be reduced when nifurtimox is combined with eflornithine, suramin, or melarsoprol.

Introduction

Nifurtimox [3-methyl-4-(5′-nitrofurfurylidene-amino)-tetrahydro-4*H*-1,4-thiazine-1,1-dioxide (nifurtimox, Bayer 2502, Lampit)] is licensed for use in Chagas disease (American trypanosomiasis), which is caused by a member of the Trypanosome genus, *Trypanosoma cruzi*. Nifurtimox also shows promise in the treatment of late-stage human African trypanosomiasis (HAT). Late-stage HAT is diagnosed by the microscopical observation of trypanosomes in the cerebrospinal fluid (CSF) and/or a white blood cell count in the CSF of >5/μl.

Current treatments for late-stage HAT include melarsoprol, which is associated with severe toxic effects, and eflornithine, which is difficult to administer and expensive to produce. A considerable advantage of nifurtimox over these existing treatments is that it is orally administered and cheap. Most importantly it has shown effectiveness in melarsoprol-refractory *Trypanosoma brucei* (*T.b.*) *gambiense* (Bisser et al., 2007).

In an attempt to improve efficacy, simplify treatment regimens, decrease toxicity, and reduce the development of drug resistance in HAT, combinations of antitrypanosomal agents are also being assessed (Bisser et al., 2007; Checchi et al., 2007; Priotto et al., 2007). A clinical trial of melarsoprol monotherapy versus combined melarsoprol-nifurtimox therapy for the treatment of CNS stage *T.b. gambiense* revealed that a consecutive 10-day low-dose combination (total melar-

This work was supported by The Wellcome Trust [Grants 073542, 080268].
Article, publication date, and citation information can be found at http://jpet.aspetjournals.org.
doi:10.1124/jpet.110.172981.

ABBREVIATIONS: HAT, human African trypanosomiasis; CNS, central nervous system; CSF, cerebrospinal fluid; BBB, blood-brain barrier; P-gp, P-glycoprotein; MRP, multidrug resistance-associated protein; p.i., postinfection; CVOs, circumventricular organs; *T.b.*, *Trypanosoma brucei*; NECT, nifurtimox-eflornithine combination therapy; ANOVA, analysis of variance; HPLC, high-performance liquid chromatography; DMSO, dimethyl sulfoxide.

soprol dose 11.4 mg/kg; total nifurtimox dose, 120 mg/kg) was more effective than the standard melarsoprol treatment (total dose 32.4 mg/kg) (Bisser et al., 2007; Woodrow et al., 2007). Unfortunately, nifurtimox in combination with melarsoprol caused excessive fatalities, and the clinical trial was terminated even though it had shown superiority over the standard melarsoprol regimes (Priotto et al., 2006; Bisser et al., 2007). A recent phase III trial examined the efficacy of nifurtimox-eflornithine combination therapy (NECT) compared with eflornithine monotherapy and discovered that, although they were noninferior to each other, NECT was less toxic, easier to administer (i.e., infusion every 12 h for 7 days versus every 6 h for 14 days), and potentially protective against the emergence of resistant parasites (Priotto et al., 2009). That study confirmed that NECT was a suitable first-line treatment against HAT (Priotto et al., 2006, 2007; Checchi et al., 2007), and NECT was added to the World Health Organization essential medicine list in April 2009 (Yun et al., 2010). It is noteworthy that the exact method by which NECT exerts its effects remains to be identified.

Our research group has examined the characteristics of eflornithine passage across the murine blood-brain and blood-CSF barriers and discovered that by combining eflornithine with suramin (a first-stage drug) the brain delivery of eflornithine was significantly improved (Sanderson et al., 2008). This would explain the improved efficacy of eflornithine-suramin combinations over monotherapy in curing CNS animal models of *T.b. rhodesiense* and *T.b. brucei* infections (Clarkson et al., 1984; Bacchi et al., 1987,1994). We have also revealed that pentamidine (another first-stage drug) can cross the BBB, but is removed by ATP binding cassette transporters including P-glycoprotein (P-gp) and MRP (Sanderson et al., 2009). This suggests that a fruitful line of research may be to optimize the CNS delivery of pentamidine and other diamidines by coadministration with P-gp and MRP inhibitors. It is therefore timely that an evaluation of the ability of nifurtimox to cross the blood-brain and blood-CSF barriers is performed.

In this study we used the in situ brain/choroid plexus perfusion method combined with capillary depletion, HPLC analyses, and the isolated incubated choroid plexus technique. The former model allows an investigation of drug transport across both blood-brain and blood-CSF barriers in parallel and in the absence of systemic metabolic enzymes. In addition, the characteristics of any drug interactions can be explored. By using the method in mice that do not express specific transporters we can gain an understanding of transporter involvement in CNS drug distribution. This brain/choroid plexus perfusion technique can also be combined with a murine model of late-stage HAT to investigate the effect of trypanosome infection on CNS drug delivery (Sanderson et al., 2008, 2009). Furthermore, an evaluation of the effect of trypanosome infection on BBB pathophysiology using this unique combination of methods has already been described (Sanderson et al., 2008). The isolated incubated choroid plexus method allows the assessment of drug accumulation at the blood-CSF barrier and, in particular, assessment of drug-transporter interactions at the apical or CSF-facing side of this blood-CNS interface. This is of special interest in *Trypanosoma brucei* infections, because the early localization of the parasites to the circumventricular organs (especially choroid plexuses), meninges, and CSF has been reported (Jennings and Gray, 1983; Mulenga et al., 2001).

Materials and Methods

Materials. Nifurtimox (molecular weight 287.30) was custom-labeled with tritium (3 and 4 position of furam ring specific activity: 2 Ci/mmol) by Moravek Biochemicals (Brea, CA). [^{14}C]sucrose (4980 mCi/mmol) was purchased from Moravek Biochemicals. Unlabeled suramin, eflornithine, and pentamidine isethionate sodium salt were purchased from Sigma-Aldrich (Dorset, UK). Unlabeled nifurtimox and melarsoprol were a kind gift from Professor S. Croft (London School of Hygiene and Tropical Medicine, London, UK).

Animals. All experimental procedures were performed according to the provisions of the United Kingdom Animals (Scientific Procedures) Act of 1987 and specified animal pathogen order (1998). Adult male BALB/c mice were purchased from Harlan (Oxon, UK). Adult FVB-Mdr1a/1b(+/+) and FVB-Mdr1a/1b(−/−) mice were imported from Taconic Farms (Germantown, NY). A breeding colony was established at King's College London, and the genotype was confirmed by polymerase chain reaction analysis (Harlan). Dr. Alfred Schinkel of the Netherlands Cancer Institute (Amsterdam, The Netherlands) is the creator of the Mdr1a/1b mice. All animals were maintained under standard conditions of temperature and lighting and given food and water ad libitum.

In Situ Brain/Choroid Plexus Perfusion Technique. The in situ brain/choroid plexus perfusion technique was carried out as described previously (Sanderson et al., 2007). In brief, adult mice (~25g) were anesthetized (2 mg/kg i.p. medetomidine hydrochloride and 150 mg/kg ketamine) and heparinized (100 U i.p.). The mice were perfused at a flow rate of 5 ml/min with oxygenated artificial plasma (Sanderson et al., 2007) by inserting a catheter into the left ventricle of the heart. With the start of perfusion an incision was made in the right atrium of the heart to prevent recirculation of perfused artificial plasma. Perfusion times were 2.5, 5, 10, 20, or 30 min. After perfusion a cistern magna CSF sample was taken and weighed, the animal was decapitated, and the brain was removed.

Brain Dissection. Cerebral cortex, caudate putamen, hippocampus, hypothalamus, thalamus, pons, cerebellum, pituitary gland, pineal gland, and IVth ventricle choroid plexus samples were taken by using a Leica (Wetzlar, Germany) S4E stereozoom microscope and weighed on a Cahn C-33 microbalance (Thermo Fisher Scientific, Waltham, MA). These regions were selected to determine drug concentration in areas affected by the trypanosome (Sanderson et al., 2007). Samples were then dissolved using 0.5 ml of Solvable (PerkinElmer Life and Analytical Sciences, Waltham, MA) for 48 h. Scintillation fluid (3.5 ml; Lumasafe; PerkinElmer Life and Analytical Sciences) was added to quantify the radioactivity of all regions of the brain before being counted using a Packard Tri-Carb 2900 TR scintillation counter with ultra low-level count mode software (PerkinElmer Life and Analytical Sciences).

Capillary Depletion Analysis. After every experiment the remaining brain after dissection was weighed and homogenized in a glass homogenizer with (×3 brain weight) in capillary depletion buffer followed by (×4 brain weight) in 26% dextran (molecular weight 60,000–90,000) as described previously (Sanderson et al., 2007). The final brain homogenate had a dextran concentration of 13%. A sample of the homogenate was retained, and the remaining homogenate was centrifuged (5400*g* for 15 min at 4°C). This produced a capillary endothelial cell-enriched pellet and parenchyma-containing supernatant. Solvable (0.5 ml for the supernatant and 0.25 ml for the pellet sample) and liquid scintillation fluid was added to the homogenate, pellet, and supernatant and was counted using the scintillation counter.

Multiple-Time Perfusion Experiments. Brain/choroid plexus perfusions were performed, as described above, in BALB/c mice. [^{3}H]nifurtimox (1.25 μM, final concentration) and [^{14}C]sucrose (1.0

μM, final concentration) were infused into the inflowing artificial plasma via a slow drive syringe pump for 2.5, 5, 10, 20, and 30 min.

In Situ Brain/Choroid Plexus Perfusion in Infected Model. The murine model of late-stage HAT is well established in outbred CD-1 mice (Jennings and Gray, 1983; Jennings et al., 2002). In our studies we chose to use the inbred BALB/c mouse strain, which is also highly susceptible to trypanosome infection (Schultzberg et al., 1988; Namangala et al., 2000; Sanderson et al., 2008, 2009) and is commonly used in studies examining the molecular and functional characterization of transporters (van Montfoort et al., 2002). Furthermore, inbred strains versus outbred stocks should reduce any animal to animal variation and consequently improve reproducibility and sensitivity of the method. Ultimately, the phenotypic uniformity of an isogenic strain means that sample size can be reduced in comparison with the use of outbred stocks.

BALB/c mice were infected with an intraperitoneal injection of 2×10^4 trypanosomes diluted in 0.1 ml of phosphate-buffered saline containing glucose, pH 8.0 as described previously (Sanderson et al., 2008). In BALB/c mice, the CNS stage of the disease is reached at ~day 11 postinfection (p.i.), and the average survival time is 37.9 ± 1.2 days (Sanderson et al., 2008). At days 7, 21, 28, and 35 p.i., individual groups of five animals were in situ brain/choroid plexus-perfused, as described above, with [^{3}H]nifurtimox (1.25 μM) and [^{14}C]sucrose (1.0 μM) for 30 min.

P-gp-Deficient Mice. P-gp deficient mice [FVB-Mdr1a/Mdr1b(−/−)] and wild-type mice [FVB-Mdr1a/Mdr1b(+/+)] were used to investigate the influence of P-gp in the efflux of [^{3}H]nifurtimox and [^{14}C]sucrose. Mice were in situ brain/choroid plexus-perfused, as described previously, for 10 min.

Inhibition Studies. Inhibition studies were carried out to determine whether [^{3}H]nifurtimox distribution into the CNS was affected by additional antitrypanosomal drugs at clinically relevant concentrations [i.e., comparable with those measured in the plasma of treated patients and also our previous published studies (Sanderson et al., 2007, 2008, 2009)] or transporter inhibitors. For these experiments, [^{3}H]nifurtimox and [^{14}C]sucrose were perfused into BALB/c mice for 10 min along with unlabeled 6 μM nifurtimox (Gonzalez-Martin et al., 1992), 30 μM melarsoprol, 150 μM suramin (Milord et al., 1993), 10 μM pentamidine (Waalkes and DeVita, 1970), 250 μM eflornithine (Milord et al., 1993), or 10 μM indomethacin, an MRP inhibitor (Huai-Yun et al., 1998). Unlabeled pentamidine, melarsoprol, nifurtimox, and indomethacin required dissolution in DMSO. The final DMSO concentration in the artificial plasma was 0.05%. Control groups were provided by [^{3}H]nifurtimox and [^{14}C]sucrose CNS distribution being examined in the presence of 0.05% DMSO.

Expression of Results. After radioactive counting, the concentration of ^{3}H or ^{14}C radioactivity in the tissue (tissue regions, homogenate, supernatant or pellet; C_{Tissue}; dpm/g) was expressed as a percentage of the concentration of radioactivity in the artificial plasma (C_{Plasma}; dpm/ml) and termed R_{Tissue} (ml · 100 g^{-1}). Brain unidirectional transfer constant, K_{in}, values can be determined from multiple-time uptake data (2.5–30 min) by means of the following relationship: $C_{\text{Tissue}}(T)/C_{\text{plasma}}(T) = K_{\text{in}}\ T + V_{\text{i}}$, where T is the perfusion time in minutes, and V_{i} is the initial volume of distribution of the test solute in the rapidly equilibrating space, which may include the vascular space, the capillary endothelial volume, and/or compartments in parallel with the BBB. The equation defines a straight line with a slope K_{in} (ml · min^{-1} · g^{-1}) and an ordinate intercept V_{d} or initial volume of distribution. Single-time uptake analysis can also be used to determine the transfer constant, $K_{\text{in}} = R_{\text{Tissue}}$/perfusion time. Where stated the R_{Tissue} results have been corrected for vascular space by subtracting the R_{Tissue} of [^{14}C]sucrose from the R_{Tissue} of [^{3}H]nifurtimox.

Isolated Incubated Choroid Plexus Method. An isolated incubated choroid plexus technique was also used to examine [^{3}H]nifurtimox and [^{14}C]sucrose accumulation from an artificial CSF into the choroid plexus tissue (Sanderson et al., 2007). Adult FVB-Mdr1a/Mdr1b(+/+) mice were anesthetized and heparinized as described above, and they were perfused through the left ventricle of the heart with artificial plasma for 4 min. The right atrium was sectioned to allow outflow of the artificial plasma. The animal was then decapitated, and the brain was removed. The IVth ventricle choroid plexus was removed and incubated in warm (37°C) artificial CSF (Gibbs and Thomas, 2002) for 10 min, followed by a 2.5-min incubation in which [^{3}H]nifurtimox (1.5 μM) and [^{14}C]sucrose (1.5 nM) were also present. The tissue was then removed and weighed on a Cahn C-33 microbalance. The choroid plexus was solubilized in 0.5 ml of Solvable (PerkinElmer Life and Analytical Sciences) over 24 h and taken with samples of the incubation medium (artificial CSF) for liquid scintillation counting. The levels of radioactivity in the choroid plexus (dpm/g) were measured as a ratio of the concentration in the artificial CSF (dpm/ml). The association of [^{3}H]nifurtimox with the choroid plexus was corrected for the extracellular space component by subtracting the [^{14}C]sucrose ratio. Inhibition studies were also carried out to determine whether [^{3}H]nifurtimox distribution into the choroid plexuses was affected by additional drugs or inhibitors and hence indicated the presence of a transporter at this site. The choroid plexuses were incubated in the presence of 6 μM nifurtimox, 150 μM suramin, 250 μM eflornithine, 10 μM pentamidine, and 30 μM melarsoprol. Nifurtimox, pentamidine, and melarsoprol were dissolved in DMSO and diluted with artificial CSF to achieve a final concentration of 0.05% DMSO. A set of control experiments also contained 0.05% DMSO.

Statistics. Samples were grouped into brain parenchyma, capillary depletion, or circumventricular organs (CVOs) and analyzed by two-way analysis of variance using Sigma Stat software (SPSS Science Software UK Ltd, Birmingham UK). Where a significant difference was observed ($P < 0.05$) individual region/sample comparisons were made using Tukey's pairwise comparisons. All data are expressed as mean ± S.E.M.

Octanol-Saline Partition Coefficient and Protein Binding Measurements. The lipophilicity of [^{3}H]nifurtimox (0.165 μM) was measured in the form of an octanol-saline partition coefficient. Binding of [^{3}H]nifurtimox (1.25 μM) to protein in the artificial plasma and human plasma (Sigma) was assessed by ultrafiltration centrifugation (Gibbs et al., 2003). Lyophilized human plasma was reconstituted in 1 ml of deionized water. To confirm that protein had not entered the ultrafiltrate, protein concentration was determined using the Lowry method (Lowry et al., 1951) .

HPLC. Samples of arterial inflow and venous outflow were taken for HPLC analyses to ensure the integrity of [^{3}H]nifurtimox during perfusion. Arterial inflow (i.e., sample of the artificial plasma) and the venous outflow were collected and passed through nylon filter membranes (pore size 0.45 μm) before undergoing analysis on a Jasco (Essex, UK) HPLC system (Montalto et al., 2002). A 100-μl aliquot of each sample was injected onto a Hamilton PRP-X300, 7-μm (250 × 4.1 mm) column and eluted at a flow rate of 0.3 ml/min with methanol (Sigma-Aldrich) and filtered deionized water (6:4). The column elutant was mixed 1:3 with scintillation fluid (Ultima Flo M; Packard, Pangbourne, UK) in a radioactive detector (Packard), and real-time analysis of radioactivity was carried out for 35 min.

In Vitro Stability Incubations. The effect of brain membrane-associated enzymes on the degradation of nifurtimox was examined over 3 h at 37°C (Thomas et al., 1997). Adult BALB/c mice were anesthetized as described earlier, and twice-washed membranes were prepared from whole brains (minus the cerebellum) as described previously (Gillespie et al., 1992). Brain homogenate was suspended in 50 mM Tris buffer to a final protein concentration of 3.51 mg/ml and frozen until use. The protein content of the suspension was confirmed by the Folin-Lowry procedure. The time course of metabolism was investigated by incubating the brain membrane homogenate with 1 mM nifurtimox at 37°C for 15, 60, 90, 120, 150, and 180 min. After incubation, an equal volume of acetonitrile was added and the samples were vortexed before being kept on ice for a

few minutes. Samples were further diluted with 0.5% acetic acid to prevent any enzymatic degradation not stopped by the addition of acetonitrile and centrifuged at 13,000*g* for 15 min. The supernatants were collected and analyzed by HPLC, as described above. The half-life of the test compound was calculated by linear regression analysis of nifurtimox recovery versus time (Thomas et al., 1997).

Results

Figure 1A shows the concentration of [^{14}C]sucrose present in select brain regions relative to the concentration in the plasma. [^{14}C]sucrose R_{Tissue} values are low at all time points in all the brain tissue samples, as we would expect if the integrity of the BBB was maintained, and significantly increase with perfusion time after allowing for the effects of differences in brain region ($P \leq 0.001$ for the brain regions including frontal cortex, occipital cortex, caudate putamen, hippocampus, hypothalamus, thalamus, pons, and cerebellum; two-way ANOVA). There was a significant difference between the [^{14}C]sucrose values ($P \leq 0.001$; two-way ANOVA) in the different brain regions after allowing for effects of differences in time, with the pons having the highest vascular space ($P < 0.01$ against all other regions; Tukey's multiple comparison) and the occipital cortex, caudate putamen, hippocampus, and thalamus having the lowest vascularities (with at least $P < 0.05$ for each specified region in this group against the other regions not specified; Tukey's multiple comparison). The initial volumes of distribution (V_d) for [^{14}C]sucrose were 3.3 ± 0.4, 1.9 ± 0.2, and

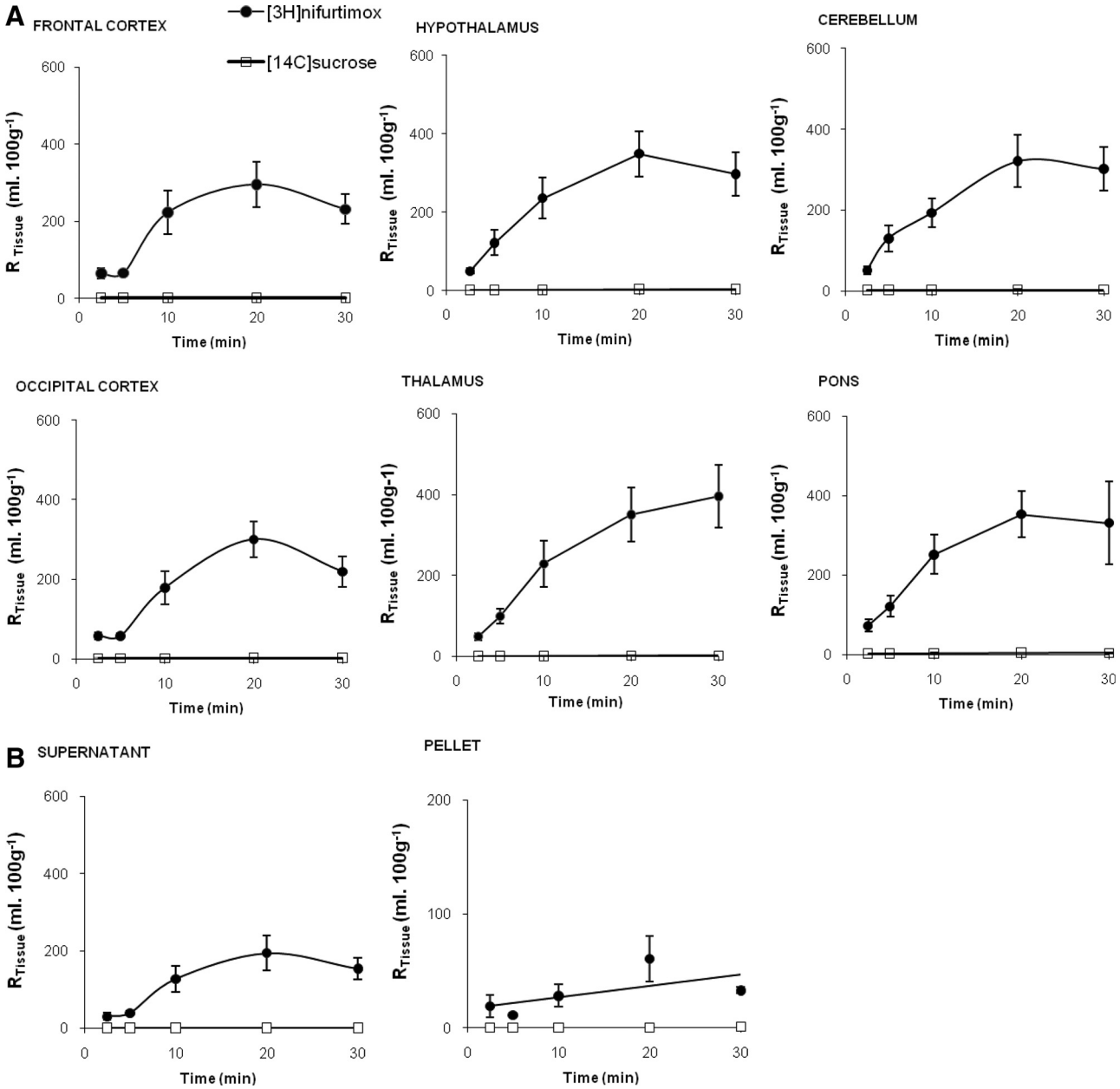

Fig. 1. A, the percentage of [^{3}H]nifurtimox and [^{14}C]sucrose detected in selected brain regions, relative to that in the artificial plasma plotted against perfusion times. Data are not shown for caudate putamen and hippocampus. B, the percentage of [^{3}H]nifurtimox and [^{14}C]sucrose detected in capillary depletion samples relative to that in the artificial plasma plotted against perfusion times. Supernatant and pellet were obtained from capillary depletion analysis of brain homogenate. Data points represent the mean ± S.E.M. (n = 4–9). Brain homogenate data are not shown.

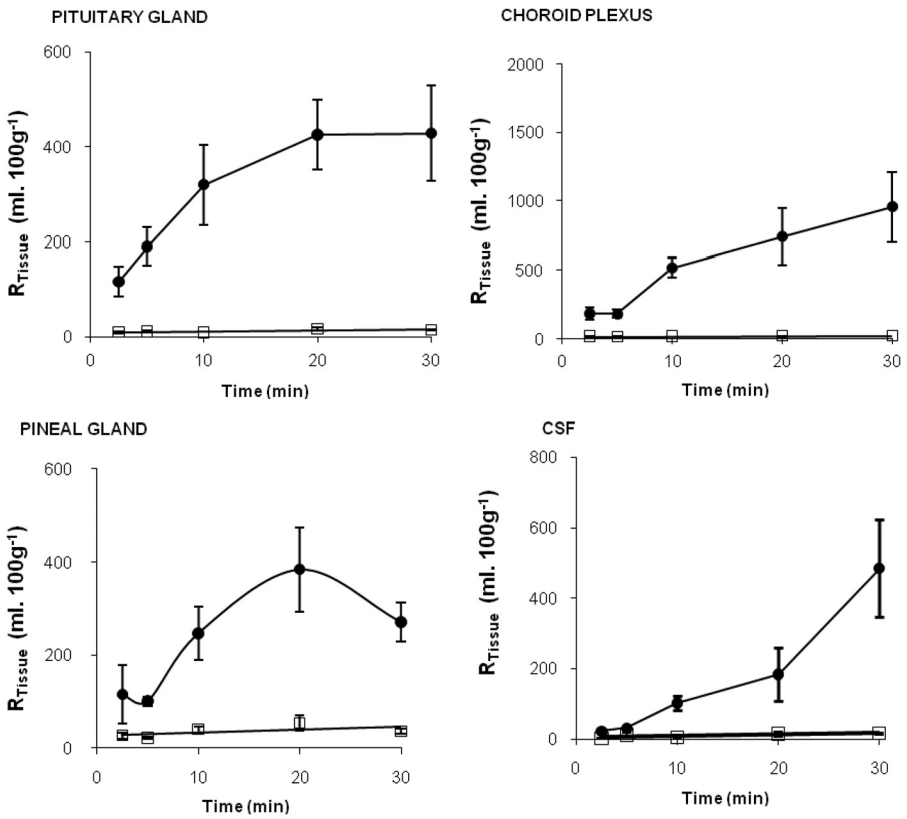

Fig. 2. The percentage of [^{3}H]nifurtimox and [^{14}C]sucrose detected in pituitary gland (top left), pineal gland (bottom left), choroid plexus (top right), and CSF (bottom right) relative to that in the artificial plasma plotted against perfusion times. Data points represent the mean ± S.E.M. (n = 4–9).

1.0 ± 0.2 ml · 100 g^{-1} for the pons, frontal cortex, and thalamus, respectively. The pons and thalamus represent the highest and one of the lowest distributions, respectively, achieved for [^{14}C]sucrose and are presented together with the frontal cortex data, a brain region that was detailed in earlier studies by our research group examining antitrypanosomal drugs (Sanderson et al., 2007, 2008, 2009). The unidirectional transfer constants (K_{in}) as determined by multiple-time uptake analysis for [^{14}C]sucrose into the pons, frontal cortex, and thalamus were 0.56 ± 0.22 (n = 28), 0.22 ± 0.10 (n = 31), and 0.56 ± 0.11 (n = 30) μl · min^{-1} · g^{-1}, respectively.

Single-time uptake analysis for [^{3}H]nifurtimox after a 2.5-min perfusion revealed a K_{in} of 251.8 ± 53.8 (n = 5), 283.1 ± 49.6 (n = 4), and 191.36 ± 36.2 (n = 5) μl · min^{-1} · g^{-1} into the pons, frontal cortex, and thalamus, respectively. It must be noted that although the two-way ANOVA on ranked data indicated a significant difference in the distribution of [^{3}H]nifurtimox ([^{14}C]sucrose space corrected) between the brain regions after allowing for the effects of differences in time (P = 0.032), the multiple comparison procedure could not identify the specific regions involved (Fig. 1A). There was a significant increase in the R_{Tissue} percentage values for [^{3}H]nifurtimox ([^{14}C]sucrose space corrected) with time (two-way ANOVA; $P \leq 0.001$). Analysis by Tukey's test revealed that this was significant between all time points ($P < 0.05$) except between the 20- and 30-min time points, which were 293.9 ± 58.4 and 229.3 ± 38.7%, respectively, in the frontal cortex ($P > 0.05$). The [^{3}H]nifurtimox ([^{14}C]sucrose space corrected) distribution was significantly higher in the homogenate ($P < 0.001$) and supernatant ($P < 0.001$) compared with the pellet (Tukey's multiple comparison procedure; Fig. 1B). There was a significantly higher accumulation of [^{3}H]nifurtimox ([^{14}C]sucrose space corrected) in the supernatant sample ($P < 0.001$), but not the pellet sample (P = 0.275), at 30 min compared with 2.5 min (two-way ANOVA on ranked data with Tukey's). There was no difference in the accumulation of [^{3}H]nifurtimox ([^{14}C]sucrose space corrected) in the supernatant between the 10-, 20-, and 30-min time points. The unidirectional transfer constants for [^{3}H]nifurtimox determined by single-time point analysis at 30 min were 64.5 ± 7.1 (n = 5), 50.8 ± 9.0 (n = 5), and 10.6 ± 1.0 (n = 5) μl · min^{-1} · g^{-1} for the homogenate, supernatant, and pellet samples, respectively.

[^{14}C]sucrose values in the CVOs (choroid plexus, pituitary, and pineal glands) did not change from the 2.5- to 30-min time point ($P > 0.05$; two-way ANOVA on ranked data; Fig. 2). [^{3}H]nifurtimox distributions ([^{14}C]sucrose space corrected) at the 10-min time points were not significantly different from those at the 20-min (P = 0.295) or 30-min (P = 0.759) time points in the CVOs. [^{3}H]nifurtimox could be detected in the CSF at all time points and reached 22.2 ± 4.4% after just 2.5-min perfusion (Fig. 2).

HPLC analysis of the arterial inflow and venous outflow samples confirmed that intact, radiolabeled nifurtimox was exposed to the luminal membranes of the blood-brain and blood-CSF barriers. The recovery of intact nifurtimox in twice-washed mouse brain membrane homogenates was plotted as a function of time (see Fig. 3), and the half-life of nifurtimox was determined to be 114 min.

Perfusions with [^{3}H]nifurtimox in a Murine Model of Sleeping Sickness. Noninfected mice (control) and mice infected with *T.b. brucei* were perfused with [^{3}H]nifurtimox on days 7, 21, 28, and 35 p.i. (Fig. 4). The distribution of [^{14}C]sucrose into the brain regions was significantly higher at 35 days compared with data from the noninfected controls ($P < 0.001$), 7 days p.i. ($P < 0.001$), 21 days p.i. ($P < 0.001$),

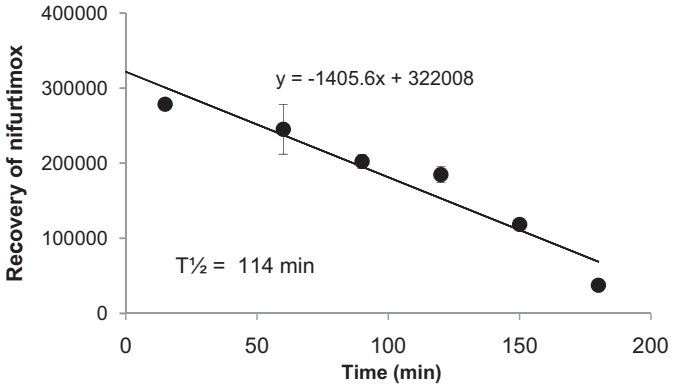

Fig. 3. The recovery of nifurtimox measured using HPLC analysis during a 3-h incubation period in twice-washed mouse brain membranes (n = 3–5 for each time point) is shown.

and 28 days p.i. ($P < 0.001$) (two-way ANOVA on the ranked data followed by Tukey). This altered [^{14}C]sucrose permeability was also observed in our earlier studies with this murine model of late-stage HAT(Sanderson et al., 2008). In contrast, the brain distribution of [^{3}H]nifurtimox was not significantly affected by the infection ($P = 0.097$; two-way ANOVA) at any time point p.i. after allowing for the effects of regional differences.

Perfusion of [^{3}H]nifurtimox in P-gp-Deficient Mice. FVB wild-type and P-gp-deficient mice were perfused for 10 min. Figure 5 shows the distribution of [^{3}H]nifurtimox ([^{14}C]sucrose/vascular space corrected) in the various brain regions and the capillary depletion analysis samples. The results indicate that there is no significant difference in the distribution of [^{3}H]nifurtimox ([^{14}C]sucrose corrected) between the control and the P-gp-deficient mice in the brain regions ($P = 0.055$), the capillary depletion analysis samples ($P = 0.341$), and the CVOs ($P = 0.118$) (two-way ANOVA).

Inhibition Studies: Perfusion of [^{3}H]nifurtimox with Unlabeled Drugs. A series of self- and cross-inhibition studies were conducted to assess whether unlabeled drugs had an effect on the ability of [^{3}H]nifurtimox to reach the CNS. Two-way ANOVA was performed on ranked data that were grouped depending on the presence of 0.05% DMSO in the artificial plasma. Therefore, [^{3}H]nifurtimox 10-min perfusions were compared with experiments that had additional concentrations of eflornithine or suramin present, and DMSO-containing [^{3}H]nifurtimox 10-min perfusions were compared with those groups of experiments that also had nifurtimox, melarsoprol, pentamidine, and indomethacin present. The brain distribution of sucrose-corrected [^{3}H]ni-

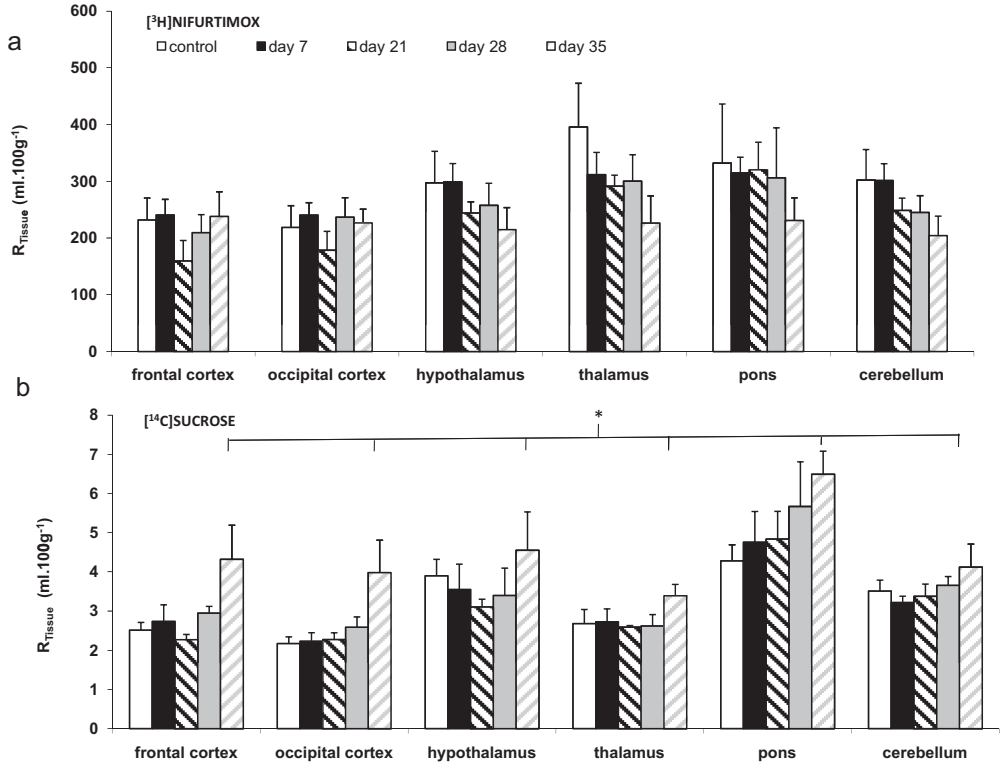

Fig. 4. The effect of *T. b. brucei* infection on the R_{Tissue} values for [^{3}H]nifurtimox (a) and [^{14}C]sucrose (b) in the brain regions. BALB/c mice were infected intraperitoneally with 2×10^4 trypanosomes and in situ-perfused on days 7, 21, 28, and 35 p.i. and compared with noninfected control mice. All data points represent the mean ± S.E.M. (n = 4–5 for each infected group and n = 9 for noninfected control). The difference in the mean values for [^{14}C]sucrose among the different postinfection groups was greater than would be expected by chance after allowing for the effects of differences in brain region (*$P \leq 0.001$; two-way ANOVA). A Tukey's multiple comparison test indicated that overall the day 35 p.i. group was significantly different from the noninfected control group ($P < 0.001$), day 7 p.i. group ($P < 0.001$), day 21 p.i. group ($P < 0.001$), and day 28 p.i. group ($P < 0.001$). The significant variation in the overall distribution of [^{14}C]sucrose to the different brain regions after allowing for the effects of infection was as reported for the multiple time uptake data ($P \leq 0.001$; two-way ANOVA). Overall, there was no significant difference in the mean values for [^{3}H]nifurtimox among the different infection groups after allowing for the effects of differences in brain region ($P < 0.097$). In contrast, there was difference for [^{3}H]nifurtimox ($P = 0.001$) distribution to the different brain regions, and the pairwise multiple comparison procedure indicated that [^{3}H]nifurtimox distribution to the thalamus was significantly larger than that found in the caudate putamen ($P < 0.003$), frontal cortex ($P < 0.031$), and hippocampus ($P < 0.043$), but not significantly different from any of the other brain regions. Data are not shown for caudate putamen and hippocampus.

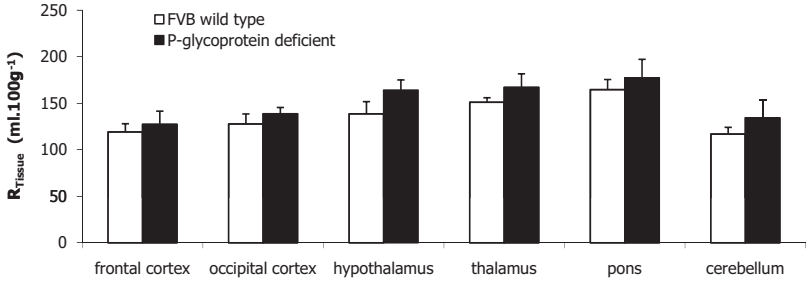

Fig. 5. [^{14}C]sucrose-corrected uptake of [^{3}H]nifurtimox in selected brain regions of FVB-Mdr1a/1b(+/+) (wild type) compared with FVB-Mdr1a/1b(−/−) (P-gp deficient) mice. Perfusion time was 10 min. Each data point shows $n = 4–6$. Data are not shown for caudate putamen, hippocampus and CVOs (choroid plexuses, pituitary gland, and pineal gland).

furtimox was significantly decreased by the presence of both unlabeled suramin ($P < 0.001$) and eflornithine ($P < 0.001$) (Tukey's multiple comparison test; [^{3}H]nifurtimox alone compared with the additional test drugs groups; Fig. 6). It is noteworthy that the [^{14}C]sucrose-corrected brain distribution of [^{3}H]nifurtimox was also significantly reduced by both melarsoprol ($P < 0.001$) and indomethacin ($P < 0.001$) (Fig. 7). However, unlabeled pentamidine caused a significant increase in the distribution of [^{3}H]nifurtimox into all the brain regions ($P < 0.001$), and 6 μM unlabeled nifurtimox had no significant effect (Fig. 7). These effects of the unlabeled drugs on [^{14}C]sucrose corrected [^{3}H]nifurtimox were also observed in the capillary depletion samples (Figs. 6 and 7). The distribution of [^{14}C]sucrose-corrected [^{3}H]nifurtimox (DMSO absent or present as appropriate) into the CVOs was affected by the presence of unlabeled suramin ($P < 0.001$) and pentamidine ($P < 0.001$), but not unlabeled nifurtimox, eflornithine, melarsoprol, and indomethacin.

Isolated Incubated Choroid Plexus Studies. Figure 8 shows the results obtained from the incubated choroid plexus studies and illustrates the absence of any significant effect on [^{3}H]nifurtimox accumulation when additional antitrypanosomal agents were added to the incubation media.

Octanol-Saline Partition Coefficient and Protein Binding. The octanol-saline partition coefficient for [^{3}H]nifurtimox was 5.46 ± 0.03. A small percentage of [^{3}H]nifurtimox was found bound to bovine serum albumin in artificial plasma (6.2 ± 1.4% bound). Approximately 38.9 ± 0.5% of nifurtimox was bound to the protein in human plasma.

Discussion

Nifurtimox is a 5-nitrofuran derivative described chemically as 3-methyl-4-(5′-nitrofurfurylidene-amino)-tetrahydro-4*H*-1,4-thiazine-1,1-dioxide that has been approved to treat HAT (Yun et al., 2010). Nifurtimox HAT treatment involves oral administration (5 mg/kg) three times a day for 14 to 21 days (Bisser et al., 2007). It is known that nifurtimox given orally (15 mg/kg) produces a maximum serum concentration of 2.6 μM in healthy volunteers (Gonzalez-Martin et al., 1992). Its toxicity includes neurological dysfunctions (Pépin et al., 1992), which is sugges-

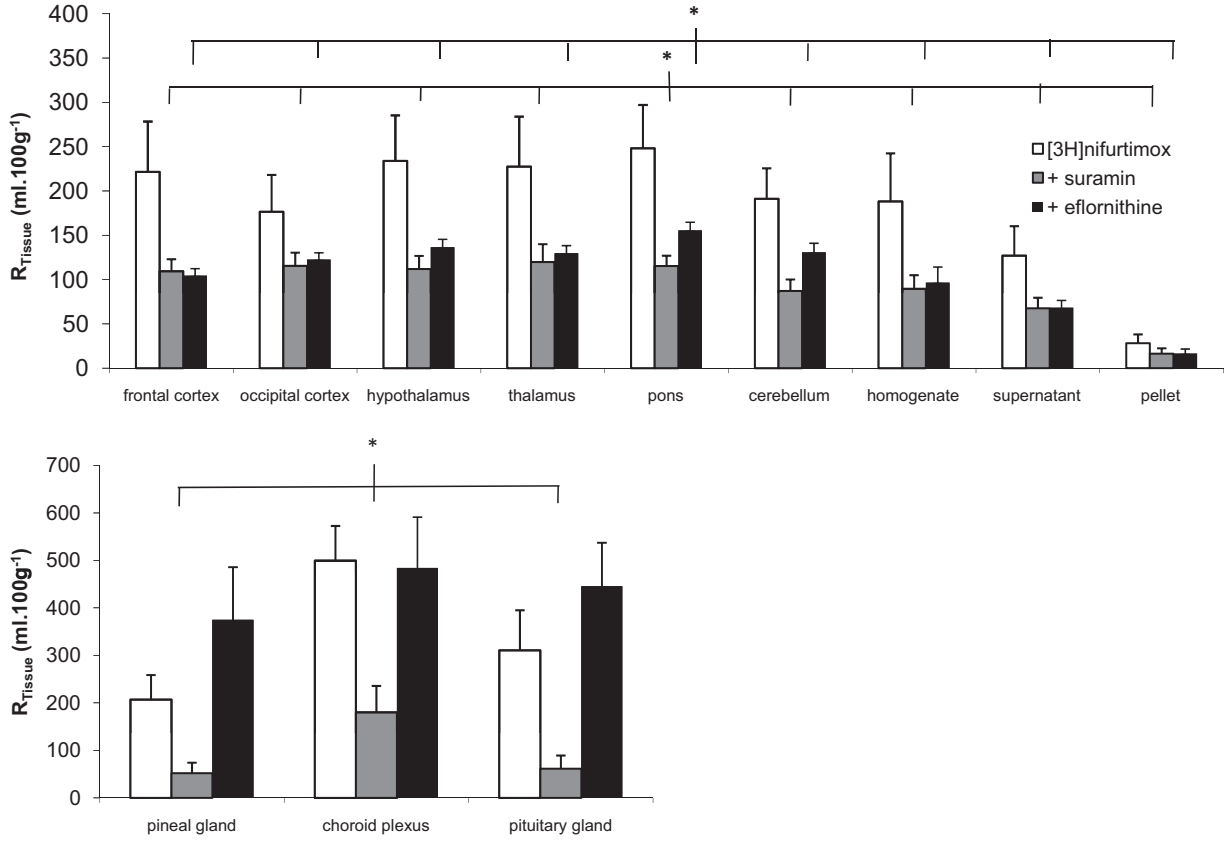

Fig. 6. The effect of 150 μM unlabeled suramin or 250 μM eflornithine on the [^{14}C]sucrose-corrected uptake of [^{3}H]nifurtimox in BALB/C mice (each group $n = 4–7$). *, $P < 0.001$ compared with [^{3}H]nifurtimox alone (two-way ANOVA). Data are not shown for caudate putamen and hippocampus.

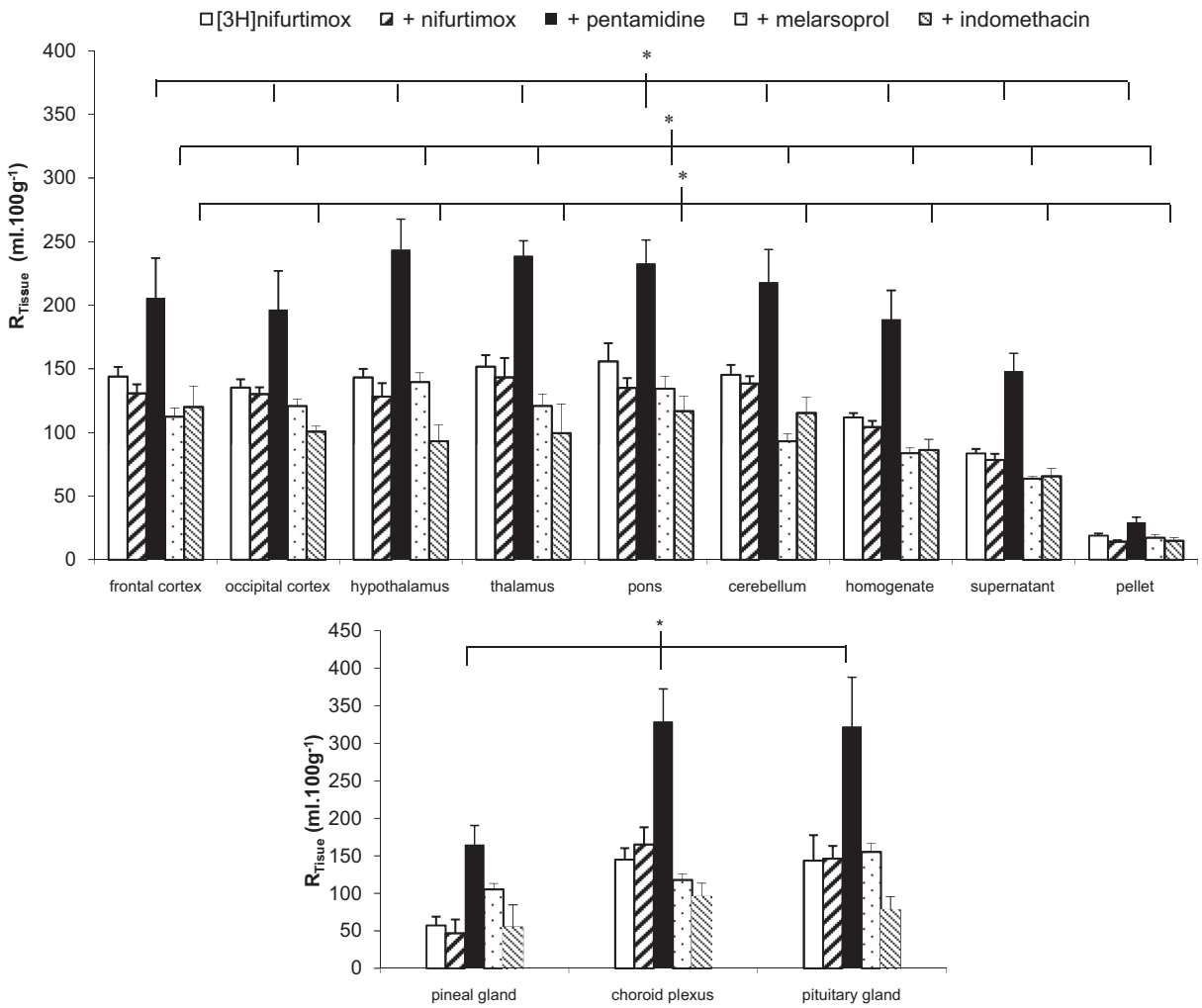

Fig. 7. The [^{14}C]sucrose-corrected CNS distribution of [^{3}H]nifurtimox in the absence and presence of 6 μM nifurtimox, 30 μM melarsoprol, 10 μM pentamidine, and 10 μM indomethacin (DMSO present). Each group shows $n = 4–5$. The overall difference in the different experimental group is greater than would be expected by chance after allowing for effects of differences in region (*, $P \leq 0.001$; two-way ANOVA). Tukey's test on these groups revealed a significant difference between each individual experimental group with [^{3}H]nifurtimox alone (each unlabeled drug group compared with the [^{3}H]nifurtimox-alone group; $P < 0.001$). Data are not shown for caudate putamen and hippocampus.

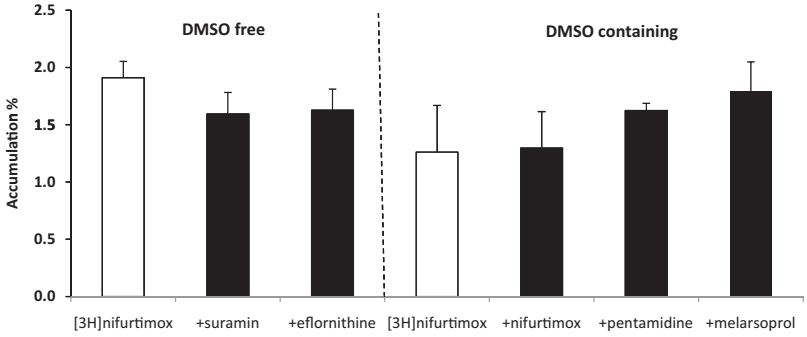

Fig. 8. The accumulation of [^{3}H]nifurtimox by the isolated incubated choroid plexus was corrected for extracellular space, as measured by [^{14}C]sucrose. Values are means ± S.E.M., and each point represents three to five mice. Two-way ANOVA was used to compare [^{3}H]nifurtimox in the absence and presence of DMSO (as appropriate) and unlabeled antitrypanosomal drugs in FVB-Mdr1a/1b(+/+) mice. No significant differences were observed.

tive of delivery to the CNS. Our results from in situ brain/choroid plexus perfusion, stability, and HPLC analyses also suggest that intact [^{3}H]nifurtimox (1.25–6 μM) can cross the blood-brain and blood-CSF barriers readily and is likely to attain concentrations in the frontal cortex (6.0 μM) and CSF (12 μM) after 30 min of perfusion that could be affective against *T.b. gambiense* (IC_{50} 1.7 μM) (Maina et al., 2007) and *T.b. rhodesiense* (IC_{50} 1.5 μM) (Baliani et al., 2005). A study in rats indicated that intravenously administered [^{35}S]nifurtimox was rapidly distributed throughout the whole organism with "relatively high" concentrations in the brain as measured by autoradiography after 2 min (Duhm et al., 1972). Further studies using a pregnant rat also revealed that the placental barrier was permeable to [^{35}S]nifurtimox and/or its metabolites. In this study the half-life for nifurtimox in mouse brain membrane homogenates was approximately 115 min. In healthy subjects

nifurtimox has a plasma half-life of 57 min (Gonzalez-Martin et al., 1992). The rapid delivery to the CNS is probably related to the high lipid solubility characteristics of [^{3}H]nifurtimox as measured by the octanol-saline partition coefficient. This high rate of nifurtimox delivery to the CNS is further highlighted by comparing brain parenchyma (supernatant) unidirectional transfer constants (K_{in}; determined by single-time analysis at 30 min) obtained for suramin [stage 1 drug, negligible (Sanderson et al., 2007)], eflornithine [stage 2 drug; 0.52 ± 0.18 $\mu l \cdot min^{-1} \cdot g^{-1}$(Sanderson et al., 2008)], pentamidine [stage 1 drug; 0.68 ± 0.12 $\mu l \cdot min^{-1} \cdot g^{-1}$ (Sanderson et al., 2009)], and nifurtimox (50.8 ± 9.0 $\mu l \cdot min^{-1} \cdot g^{-1}$).

Our previous studies using the murine model of late-stage HAT in BALB/c mice have indicated an increase in the CNS delivery of molecules at day 35 p.i. (Sanderson et al., 2008, 2009). The largest compound that we have studied that was able to cross the infected BBB after 35 days p.i. was [^{3}H]suramin (molecular weight 1429.2), suggesting considerable loss of integrity because this molecule is highly bound to albumin (60 kDa; radius 35.5 Å) (Sanderson et al., 2007, 2009). This loss of BBB integrity at day 35 is also demonstrated in this study with [^{14}C]sucrose and is a consistent feature of this BALB/c mouse model of late-stage HAT(Sanderson et al., 2008, 2009). It is noteworthy that we also have evidence of increased permeability to [^{14}C]sucrose at day 28 (Sanderson et al., 2009). Although this was not demonstrated in a trypanosome-infected mouse study when we were coperfusing [^{14}C]sucrose (molecular weight 342) with [^{3}H]eflornithine, the integrity of the barrier to the smaller molecule [^{3}H]eflornithine (molecular weight 237) was increased at this time point (Sanderson et al., 2008). In this study we did not present any measurable changes to the integrity of the barrier to [^{14}C]sucrose at day 28 p.i. Taken together, our studies indicate that up to 21 days p.i. there is no up- or down-regulation of specific transporters (including P-gp and MRP) as measured with eflornithine, pentamidine, or nifurtimox (Sanderson et al., 2008, 2009). Furthermore, our studies are suggestive of a gradual loss of barrier integrity caused by trypanosome infection around day 28, and this loss can be consistently demonstrated at the day 35 p.i. time point in this murine model of late-stage HAT. A previous study has shown that *T. b. rhodesiense*, but not *T. b. brucei*, caused a transient change in BBB permeability as measured by transendothelial electrical resistance measurements in a human brain microvessel endothelial cell line during an overnight parasite incubation (Grab et al., 2004; Nikolskaia et al., 2008). This implies a reversible change in paracellular permeability and tight junction integrity with human trypanosome invasion of the CNS.

It is noteworthy that our study revealed the brain distribution of [^{3}H]nifurtimox remained unchanged when there was considerable loss of BBB integrity caused by the trypanosome infection at day 35 p.i. This would suggest that healthy cerebral capillary endothelial cells do not provide a significant physical barrier to the movement of [^{3}H]nifurtimox (molecular weight 287.3) into the CNS. It is also likely that [^{3}H]nifurtimox movement across the BBB predominantly depends on the transcellular pathway and not the paracellular pathway.

Although our self-inhibition studies caused no significant change to the CNS delivery of [^{3}H]nifurtimox, our cross-competition studies revealed that [^{3}H]nifurtimox may use transporters to cross the capillary endothelium with unlabeled pentamidine enhancing the brain distribution of [^{3}H]nifurtimox, suggestive of some cellular barrier restriction, possibly an efflux (brain to blood) transporter. The discrepancy between the self- and cross-inhibition results probably is linked to the relatively low concentration of unlabeled nifurtimox (6 μM) that was used in this study (see *Materials and Methods*). The presence of an efflux transporter is also indicated by the relatively low K_{in} value for nifurtimox distribution into the supernatant in relation to its high octanol-saline partition coefficient and small molecular weight. In our earlier work we demonstrated that [^{3}H]pentamidine is a P-gp substrate and there was a significant interaction between [^{3}H]pentamidine and unlabeled nifurtimox, with the CNS distribution of pentamidine being increased by the presence of unlabeled nifurtimox (Sanderson et al., 2009). It is noteworthy that verapamil, a P-gp inhibitor and substrate, reversed the nifurtimox-resistance of a strain of *T. cruzi* (Neal et al., 1989). However, in this study we found no significant [^{3}H]nifurtimox removal by P-gp as measured using P-gp-deficient mice and wild-type controls. Thus it may be that nifurtimox is an inhibitor and not a substrate of P-gp, and/or a different efflux transporter is involved in the observed interactions between [^{3}H]nifurtimox and pentamidine. A possible candidate is one of the members of the MRP family that are expressed at the BBB. However, indomethacin, an inhibitor that frequently is used to inhibit MRP (Huai-Yun et al., 1998), produced a decrease, and not an increase as was observed with the addition of pentamidine, in the brain distribution of [^{3}H]nifurtimox. [Although it is noted that indomethacin is known to inhibit other transporters such as organic anion transporter 2 (Morita et al., 2001).] Furthermore, P-gp is not densely expressed at the murine choroid plexus (Soontornmalai et al., 2006), and unlabeled pentamidine also caused a significant increase in the association of [^{3}H]nifurtimox with this tissue when it was present in the blood (Fig. 7), but no affect was observed when unlabeled pentamidine was present on the CSF side (Fig. 8). This is suggestive of an interaction of pentamidine and nifurtimox with a transporter on the blood side of the choroid plexus. The identity of this transporter remains unknown, but an interesting candidate is breast cancer resistance protein, which is expressed at the BBB and the choroid plexus (Lee et al., 2005), as well as in breast tissue, and may play a role in the active secretion of nitrofurantoin (which is chemically similar to nifurtimox) into milk (Garcia-Bournissen et al., 2010).

The higher concentration of [^{3}H]nifurtimox in the CNS compared with the plasma is also suggestive of a transporter that aids delivery of nifurtimox to the brain. It is noteworthy that a drug that caused [^{3}H]nifurtimox distribution to the brain to decrease was melarsoprol, indicative of an interaction between these two drugs. A clinical trial has demonstrated a degree of synergism between melarsoprol and nifurtimox (Bisser et al., 2007). Although we do not have evidence for a positive effect of melarsoprol on the brain distribution of nifurtimox it is possible that nifurtimox alters the concentration of melarsoprol in the brain so producing this synergy.

In light of the encouraging results of nifurtimox-eflornithine combination therapies (Bisser et al., 2007; Priotto et al., 2007), an important assessment is how [^{3}H]nifurtimox distribution to the CNS is affected by the presence of unlabeled eflornithine. It is noteworthy that eflornithine caused an approximately 53% decrease in brain (but did not affect CVO) distribution of [^{3}H]nifurtimox after 10-min exposure. Theoretically, based on these values [^{3}H]nifurtimox would still reach an effective concentration within the brain when eflornithine was present, but it must be emphasized this interaction has been measured only over a short time period.

Because [^{3}H]nifurtimox interacts with transporters at the BBB and there was a lack of any effect to [^{3}H]nifurtimox brain distribution when there was significant loss of BBB integrity because of trypanosome infection, our data would further suggest that *T.b. brucei* causes significant increases in the paracellular permeability of the BBB, while the endothelial cells themselves remain intact.

In light of unsatisfactory therapeutic options (melarsoprol, eflornithine, and nifurtimox) for second-stage sleeping sickness, combinations of existing drugs have been considered the most promising way forward to maximize cure rates and improve tolerability in the short term. Furthermore, nifurtimox monotherapy is being discouraged, because most studies have reported high treatment failure rates (Pépin et al., 1992; Bisser et al., 2007). Our study would suggest that [^{3}H]nifurtimox crosses the healthy and infected murine blood-brain and blood-CNS barriers very well. Although interactions with other antitrypanosomal drugs (including eflornithine) are indicated at the transporter level of the barriers and this may reduce final brain drug concentrations, it seems that not all combinations (i.e., nifurtimox plus pentamidine) would be detrimental to the efficacy of nifurtimox against trypanosomes within the CNS.

Authorship Contributions

Participated in research design: Rodgers and Thomas.

Conducted experiments: Jeganathan, Sanderson, and Dogruel.

Contributed new reagents or analytic tools: Croft.

Performed data analysis: Jeganathan, Sanderson, and Thomas.

Wrote or contributed to the writing of the manuscript: Sanderson and Thomas.

Other: Thomas acquired funding for the research.

References

Bacchi CJ, Nathan HC, Clarkson AB Jr, Bienen EJ, Bitonti AJ, McCann PP, and Sjoerdsma A (1987) Effects of the ornithine decarboxylase inhibitors DL-α-difluoromethylornithine and α-monofluoromethyldehydroornithine methyl ester alone and in combination with suramin against *Trypanosoma brucei brucei* central nervous system models. *Am J Trop Med Hyg* **36:**46–52.

Bacchi CJ, Nathan HC, Yarlett N, Goldberg B, McCann PP, Sjoerdsma A, Saric M, and Clarkson AB Jr (1994) Combination chemotherapy of drug-resistant *Trypanosoma brucei rhodesiense* infections in mice using DL-α-difluoromethylornithine and standard trypanocides. *Antimicrob Agents Chemother* **38:**563–569.

Baliani A, Bueno GJ, Stewart ML, Yardley V, Brun R, Barrett MP, and Gilbert IH (2005) Design and synthesis of a series of melamine-based nitroheterocycles with activity against Trypanosomatid parasites. *J Med Chem* **48:**5570–5579.

Bisser S, N′Siesi FX, Lejon V, Preux PM, Van Nieuwenhove S, Miaka Mia Bilenge C, and Büscher P (2007) Equivalence trial of melarsoprol and nifurtimox monotherapy and combination therapy for the treatment of second-stage *Trypanosoma brucei gambiense* sleeping sickness. *J Infect Dis* **195:**322–329.

Checchi F, Piola P, Ayikoru H, Thomas F, Legros D, and Priotto G (2007) Nifurtimox plus eflornithine for late-stage sleeping sickness in Uganda: a case series. *PLoS Negl Trop Dis* **1:**e64.

Clarkson AB Jr, Bienen EJ, Bacchi CJ, McCann PP, Nathan HC, Hutner SH, and Sjoerdsma A (1984) New drug combination for experimental late-stage African trypanosomiasis: DL-α-difluoromethylornithine (DFMO) with suramin. *Am J Trop Med Hyg* **33:**1073–1077.

Duhm B, Maul W, Medenwald H, Patzschke K, and Wegner LA (1972) Investigations on the pharmacokinetics of nifurtimox-35 S in the rat and dog. *Arzneimittelforschung* **22:**1617–1624.

Garcia-Bournissen F, Altcheh J, Panchaud A, and Ito S (2010) Is use of nifurtimox for the treatment of Chagas disease compatible with breast feeding? A population pharmacokinetics analysis. *Arch Dis Child* **95:**224–228.

Gibbs JE and Thomas SA (2002) The distribution of the anti-HIV drug, 2′3′-dideoxycytidine (ddC), across the blood-brain and blood-cerebrospinal fluid barriers and the influence of organic anion transport inhibitors. *J Neurochem* **80:**392–404.

Gibbs JE, Jayabalan P, and Thomas SA (2003) Mechanisms by which 2′,3′-dideoxyinosine (ddI) crosses the guinea-pig CNS barriers; relevance to HIV therapy. *J Neurochem* **84:**725–734.

Gillespie TJ, Konings PN, Merrill BJ, and Davis TP (1992) A specific enzyme assay for aminopeptidase M in rat brain. *Life Sci* **51:**2097–2106.

González-Martin G, Thambo S, Paulos C, Vásquez I, and Paredes J (1992) The pharmacokinetics of nifurtimox in chronic renal failure. *Eur J Clin Pharmacol* **42:**671–673.

Grab DJ, Nikolskaia O, Kim YV, Lonsdale-Eccles JD, Ito S, Hara T, Fukuma T, Nyarko E, Kim KJ, Stins MF, et al. (2004) African trypanosome interactions with an in vitro model of the human blood-brain barrier. *J Parasitol* **90:**970–979.

Huai-Yun H, Secrest DT, Mark KS, Carney D, Brandquist C, Elmquist WF, and Miller DW (1998) Expression of multidrug resistance-associated protein (MRP) in brain microvessel endothelial cells. *Biochem Biophys Res Commun* **243:**816–820.

Jennings FW and Gray GD (1983) Relapsed parasitaemia following chemotherapy of chronic *T. brucei* infections in mice and its relation to cerebral trypanosomes. *Contrib Microbiol Immunol* **7:**147–154.

Jennings FW, Rodgers J, Bradley B, Gettinby G, Kennedy PG, and Murray M (2002) Human African trypanosomiasis: potential therapeutic benefits of an alternative suramin and melarsoprol regimen. *Parasitol Int* **51:**381–388.

Lee YJ, Kusuhara H, and Sugiyama Y (2005) Lack of contribution of P-glycoprotein (P-gp) to transport via the mouse blood-cerebrospinal fluid barrier. *J Health Sci* **51:**101–105.

Lowry OH, Rosebrough NJ, Farr AL, and Randall RJ (1951) Protein measurement with the folin phenol reagent. *J Biol Chem* **193:**265–275.

Maina N, Maina KJ, Mäser P, and Brun R (2007) Genotypic and phenotypic characterization of *Trypanosoma brucei gambiense* isolates from Ibba, South Sudan, an area of high melarsoprol treatment failure rate. *Acta Trop* **104:**84–90.

Milord F, Loko L, Ethier L, Mpia B, and Pépin J (1993) Eflornithine concentrations in serum and cerebrospinal fluid of 63 patients treated for *Trypanosoma brucei gambiense* sleeping sickness. *Trans R Soc Trop Med Hyg* **87:**473–477.

Montalto de Mecca M, Diaz EG, and Castro JA (2002) Nifurtimox biotransformation to reactive metabolites or nitrite in liver subcellular fractions and model systems. *Toxicol Lett* **136:**1–8.

Morita N, Kusuhara H, Sekine T, Endou H, and Sugiyama Y (2001) Functional characterization of rat organic anion transporter 2 in LLC-PK1 cells. *J Pharmacol Exp Ther* **298:**1179–1184.

Mulenga C, Mhlanga JD, Kristensson K, and Robertson B (2001) *Trypanosoma brucei brucei* crosses the blood-brain barrier while tight junction proteins are preserved in a rat chronic disease model. *Neuropathol Appl Neurobiol* **27:**77–85.

Namangala B, de Baetselier P, Brijs L, Stijlemans B, Noël W, Pays E, Carrington M, and Beschin A (2000) Attenuation of *Trypanosoma brucei* is associated with reduced immunosuppression and concomitant production of Th2 lymphokines. *J Infect Dis* **181:**1110–1120.

Neal RA, van Bueren J, McCoy NG, and Iwobi M (1989) Reversal of drug resistance in *Trypanosoma cruzi* and *Leishmania donovani* by verapamil. *Trans R Soc Trop Med Hyg* **83:**197–198.

Nikolskaia OV, de ALA, Kim YV, Lonsdale-Eccles JD, Fukuma T, Scharfstein J, and Grab DJ (2008) Erratum.*J Clin Invest* **118:**1974.

Pépin J, Milord F, Meurice F, Ethier L, Loko L, and Mpia B (1992) High-dose nifurtimox for arseno-resistant *Trypanosoma brucei gambiense* sleeping sickness: an open trial in central Zaire. *Trans R Soc Trop Med Hyg* **86:**254–256.

Priotto G, Fogg C, Balasegaram M, Erphas O, Louga A, Checchi F, Ghabri S, and Piola P (2006) Three drug combinations for late-stage *Trypanosoma brucei gambiense* sleeping sickness: a randomized clinical trial in Uganda. *PLoS Clin Trials* **1:**e39.

Priotto G, Kasparian S, Mutombo W, Ngouama D, Ghorashian S, Arnold U, Ghabri S, Baudin E, Buard V, Kazadi-Kyanza S, et al. (2009) Nifurtimox-eflornithine combination therapy for second-stage African *Trypanosoma brucei gambiense* trypanosomiasis: a multicentre, randomised, phase III, non-inferiority trial. *Lancet* **374:**56–64.

Priotto G, Kasparian S, Ngouama D, Ghorashian S, Arnold U, Ghabri S, and Karunakara U (2007) Nifurtimox-eflornithine combination therapy for second-stage *Trypanosoma brucei gambiense* sleeping sickness: a randomized clinical trial in Congo. *Clin Infect Dis* **45:**1435–1442.

Sanderson L, Dogruel M, Rodgers J, Bradley B, and Thomas SA (2008) The blood-brain barrier significantly limits eflornithine entry into *Trypanosoma brucei brucei* infected mouse brain. *J Neurochem* **107:**1136–1146.

Sanderson L, Dogruel M, Rodgers J, De Koning HP, and Thomas SA (2009) Pentamidine movement across the murine blood-brain and blood-cerebrospinal fluid barriers: effect of trypanosome infection, combination therapy, P-glycoprotein, and multidrug resistance-associated protein. *J Pharmacol Exp Ther* **329:**967–977.

Sanderson L, Khan A, and Thomas S (2007) Distribution of suramin, an antitrypanosomal drug, across the blood-brain and blood-cerebrospinal fluid interfaces in wild-type and P-glycoprotein transporter-deficient mice. *Antimicrob Agents Chemother* **51:**3136–3146.

Schultzberg M, Ambatsis M, Samuelsson EB, Kristensson K, and van Meirvenne N (1988) Spread of *Trypanosoma brucei* to the nervous system: early attack on circumventricular organs and sensory ganglia. *J Neurosci Res* **21:**56–61.

Soontornmalai A, Vlaming ML, and Fritschy JM (2006) Differential, strain-specific cellular and subcellular distribution of multidrug transporters in murine choroid plexus and blood-brain barrier. *Neuroscience* **138:**159–169.

Thomas SA, Abbruscato TJ, Hau VS, Gillespie TJ, Zsigo J, Hruby VJ, and Davis TP (1997) Structure-activity relationships of a series of [D-Ala2]deltorphin I and II analogues; in vitro blood-brain barrier permeability and stability. *J Pharmacol Exp Ther* **281:**817–825.

van Montfoort JE, Schmid TE, Adler ID, Meier PJ, and Hagenbuch B (2002) Functional characterization of the mouse organic-anion-transporting polypeptide 2. *Biochim Biophys Acta* **1564:**183–188.

Waalkes TP and DeVita VT (1970) The determination of pentamidine (4,4′-diamidinophenoxypentane) in plasma, urine, and tissues. *J Lab Clin Med* **75:**871–878.

Woodrow CJ, Abel PM, and Krishna S (2007) Randomized, controlled trial of treatments for second-stage sleeping sickness. *J Infect Dis* **196:**650–651.

Yun O, Priotto G, Tong J, Flevaud L, and Chappuis F (2010) NECT is next: implementing the new drug combination therapy for *Trypanosoma brucei gambiense* sleeping sickness. *PLoS Negl Trop Dis* **4:**e720.

Address correspondence to: Dr. Sarah Ann Thomas, King's College London, Pharmaceutical Sciences Research Division, Hodgkin Building, Guy's Campus, London, SE1 1UL United Kingdom. E-mail: sarah.thomas@kcl.ac.uk